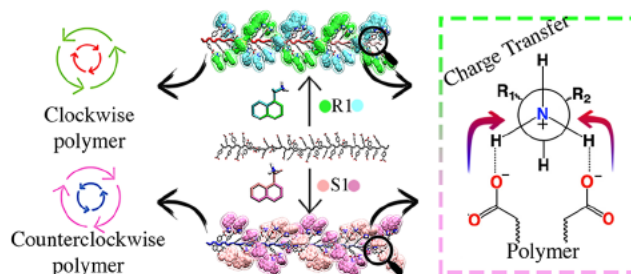


Local Electronic Charge Transfer in the Helical Induction of *Cis-Transoid* Poly(4-carboxyphenyl)acetylene by Chiral Amines

Montserrat Penaloza-Amion,* Celso R. C. Rêgo,* and Wolfgang Wenzel*

ABSTRACT: Understanding the phenomena that lead to the formation of a specific helicity in helical polymers remains a challenge even today. Various polymers have been shown to assume different helical screw senses depending on different stimuli. Acid–base chiral amines, for example, can induce helical conformations on *cis transoid* poly(4 carboxyphenyl)acetylene yielding high intensity circular dichroism signals. There have been many experimental attempts to elucidate the driving forces involved, but the induction process remains unclear. Here, we investigate the mechanism of helical polymer formation by both Molecular Dynamics (MD) and Density Functional Theory (DFT) approaches. We find that DFT calculations and the dissociation energies between 4 monomer polymers and amines show a clear trend in the affinity of *R* and *S* conformers with clockwise and counterclockwise polymer screw senses, respectively. The charge analysis revealed that the local charge transfer effect plays a crucial role that leads to the helical polymer amine induction.



I. INTRODUCTION

Helical structures are present in many natural macromolecules such as DNA and proteins. Inspired by these biomolecules, polymer scientists are highly interested to find synthesis routes and mechanisms to control helix formation in polymers. Synthetic helical polymers gained much attention for a wide range of potential applications such as chiral recognition, asymmetric catalysis, chiro optical switches,¹ and applications in the field of nanostructure material design.^{2–5} Optical activity is a fundamental property of helical polymers, making them intrinsically chiral. Helical polymers with bulky pendant groups, such as poly(methacrylate)s⁶ or poly(isocyanides)s,⁷ are governed by high steric repulsion that results in high inversion barriers. On the other hand, highly dynamic helical polymers have low inversion barriers but nevertheless exhibit optical activity. Experimental techniques such as UV, NMR, Circular Dichroism (CD), Atomic Force Microscopy (AFM), and X ray diffraction (XRD) are regularly used to demonstrate the existence of dynamic helical polymers.⁸ However, these techniques struggle to elucidate the mechanism and processes responsible for the formation of helical structures. Therefore, investigating the formation of spatial orientation of dynamic helical polymers is a question of great interest in understanding existing polymers and designing new materials and their potential application.

Poly(phenylacetylene)s (PPAs) are a family of dynamic helical polymers which are optically inactive. Historically, the first induced helical polymer (IHP) with noncovalent interacting ligands was reported by Yashima et al.^{9,10} They found that chiral amines and amino alcohols can induce a

prevailing one handedness in nonoptically active stereoregular *cis transoid* polyacetylene with 4 carboxyphenyl bearing groups (poly 1) as depicted in Figure 1. The chiral effects of the host molecules and chromophore groups are usually measured via induced CD (ICD). The IHP shows mirror CD images for each enantiomer and very characteristic CD signals for the backbone in the absorption region between 300 and 500 nm.^{8,10} The IHPs have three interesting phenomena: 1) the sergeants and soldiers principle¹¹ where a small number of chiral molecules could induce a helical conformation in some dynamic helical polymers, 2) the majority rule¹² where the screw sense of the helical polymer is induced in the presence of a mixture of two enantiomers, and 3) the memory effect¹³ where in IHP the helicity can be conserved after removing the chiral compounds and replacing them with nonchiral hosts.

While there is a considerable number of experimental publications about dynamic helical polymers^{1,8,14} and works related to the induction mechanism driven by different side chain modifications on PPAs,^{15–20} solvent influence,^{16,21} temperature,²² and pH,²³ there is still a need for a deeper understanding of the induction process. Currently, there is

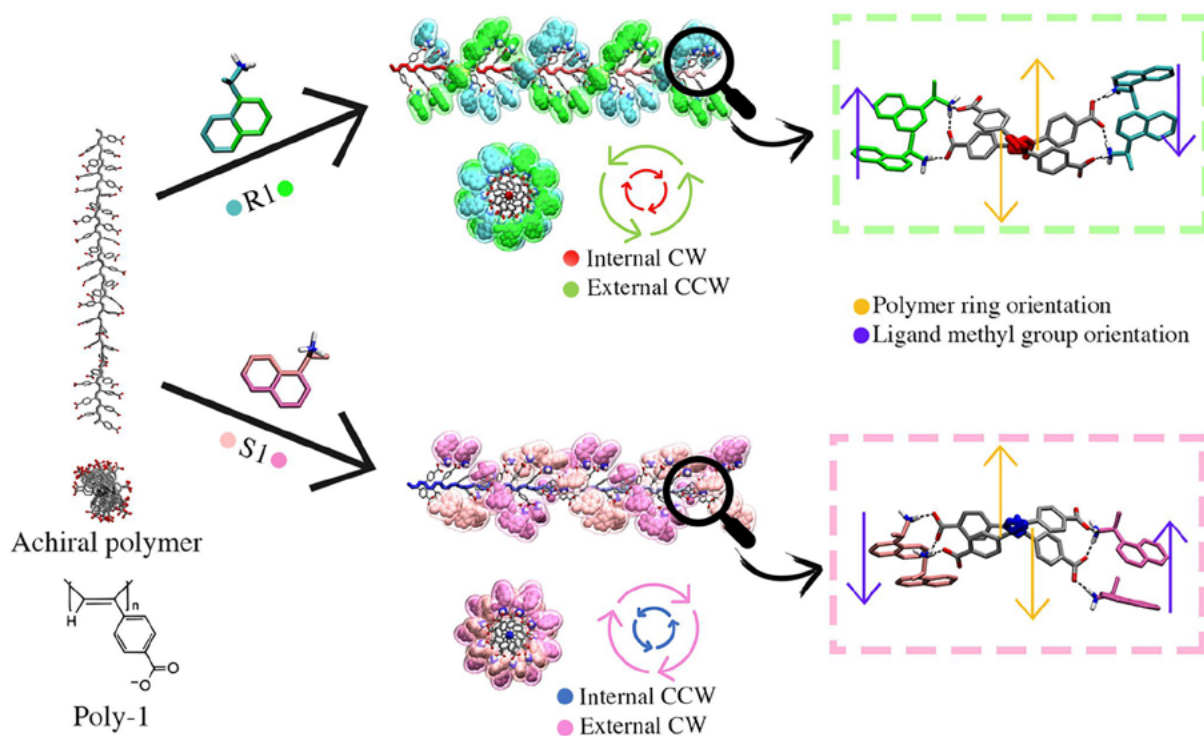


Figure 1. Scheme of helical induction of achiral poly 1 interacting with R1 and S1 chiral amines. Forty monomer helical polymer amine complexes with clockwise (CW) and counterclockwise (CCW) screw senses. They were obtained by studying the interactions with 4 monomer complex models and DFT calculations (pink and green dash boxes) with implicit solvation. R1 ligands are represented with green and cyan, while S1 ligands are represented with pink and magenta.

almost no theoretical work on induced helical polymers or on the induction mechanism.

In 1997, Yashima et al.¹⁰ attempted to evaluate the stability of poly 1 using molecular mechanics and molecular dynamics calculations with a model of 20 monomers. They created a left and right handed optimized model. In this work, they reported the existence of a helical conformation that lost its helicity after a few ps of simulation. They concluded that the reported helical conformation of poly 1 may not be stable in solution.

Here, we use complementary computational methodologies to understand physicochemical systems at a nanoscale level. Molecular Dynamics (MD) simulations based on the force field approach are convenient to study dynamical processes on helical polymers²⁴ but rely on a number of approximations regarding the force field. On the other hand, electronic structure calculations can provide useful microscopic information such as the charge transfer in simplified systems,^{25–27} regarding parameters required for MD calculations, and such as dihedral potentials²⁸ and provide valuable information regarding the binding affinity.²⁹ However, these methods are largely confined to modeling static configurations.

This work reports on the dynamic helix formation in poly 1 and sheds light on the nature of the induction mechanism in the presence of chiral compounds. We studied the interactions of (R) and (S) 1 (1-naphthyl)ethylamine (R1 and S1) investigated by Yashima et al.^{10,13} with poly 1 clockwise (CW) and counterclockwise (CCW) conformations. Using molecular mechanics and electronic structure calculations, we examine in detail polymer amine interactions and find affinity trends using Density Functional Theory (DFT) combined with a posteriori energy dispersion correction. We obtained dissociation energies of polymer amine complexes and performed Bader charge

analysis that revealed the charge transfer between the carboxylic and amine group from polymer and chiral amines.

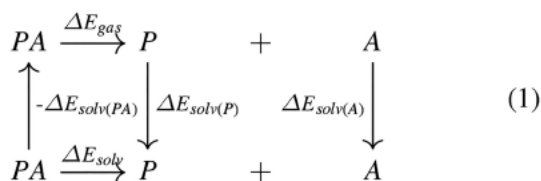
II. COMPUTATIONAL DETAILS

Density Functional Theory Calculations. As a first step, we performed an electronic structure calculation to determine favorable helix configurations. The formation of the helix is primarily controlled by the values of the backbone dihedral angles. We searched for the angles by performing scan calculations rotating them in the range 0° – 360° with steps of 10° degrees using TURBOMOLE 7.3^{30–32} with the hybrid B3LYP functional^{33,34} and def2 SV(P) basis set.³⁵ To compensate for the poor description of van der Waals (vdW) interactions by local and semilocal XC functionals,^{36,37} we employed a posteriori energy dispersion correction D3 BJ.^{38,39}

Minimal polymer amine complexes consisting of 4 monomers were constructed using the dihedral information obtained from the scan calculations to create CW and CCW conformations for poly 1, and amines were placed interacting with each carboxylic acid. Different orientations of the methyl and naphthalene groups were created to determine the lowest energy complexes. All the complexes were optimized using the same DFT setup used for the dihedral scan simulation.

The dissociation energies for R1 and S1 chiral compounds around the polymer are computed via DFT (electronic energy) using 4 monomer polymer amine complexes according to the cycle in eq 1 where PA, P, and A are the polymer amine complex, polymer, and amine, respectively.

The calculation of the dissociation energy of each amine in dimethyl sulfoxide (DMSO) (ΔE_{diss}) is equal to the energy variation ΔE_{solv} (eq 2) as defined in eq 1



$$\Delta E_{diss} = \Delta E_{solv} \quad (2)$$

According to the paths in eq 1, ΔE_{solv} is calculated by accounting for the contributions ΔE_{gas} and $\Delta\Delta E_{solv}$ as given in eq 3.

$$\Delta E_{solv} = \Delta E_{gas}(PA) + \Delta\Delta E_{solv}(PA) \quad (3)$$

Such contributions are obtained from the optimization of PA, P, and A in the gas phase and in the solvated state, and then the energy contributions are obtained as represented in eqs 4 and 5 for $\Delta E_{gas}(PA)$ and $\Delta\Delta E_{solv}(PA)$, respectively.

$$\Delta E_{gas}(PA) = E_{gas}(P) + E_{gas}(A) - E_{gas}(PA) \quad (4)$$

$$\Delta\Delta E_{solv}(PA) = \Delta E_{solv}(P) + \Delta E_{solv}(A) - \Delta E_{solv}(PA) \quad (5)$$

We computed all the states for the polymer amine complex, polymer, and amine represented in eq 1 using the same DFT configuration as in our previous studies. Solvated states in DMSO (Dielectric Constant ($\epsilon_{solvent}$) = 47) were obtained using the COSMO solvation method.⁴⁰ The dissociation, ΔE_{diss} , of the amines was calculated one by one per monomer position with CW and CCW screw senses. To evaluate the influence of the chiral center, in each complex, the chiral methyl group covalently bound to each chiral center was exchanged with the hydrogen atom to convert each monomer from R to S and S to R, respectively.

Bader Net Charge Analysis. We used the Bader analysis to estimate the partial charge for the system under study to observe the amine's influence over the polymer's charge distribution. To compute the Bader charge Q^B for every atom in the molecule, we employed VASP^{41–44} high density grids.⁴⁵ Thus, we calculated the effective charge by $\Delta Q = Z_{val} - Q^B$, where Z_{val} and Q^B are the valence electron number, extracted from the VASP POTCAR file, and Bader charge on each atom. As in this part of the protocol, we would have to submit many independent tasks for different scenarios in the CW or CCW screw sense, and to speed up the process, we managed all Bader analysis simulations by using the Workflow Active Nodes DFT VASP developed within the SimStack workflow framework.^{46,47}

We analyze the orientation of the amines in extended 40 monomer complexes to obtain the first coordinates for MD simulations. The lowest energy complexes obtained for the 4 monomer polymers with similar energy compared to CW and CCW were used to extract the relative orientation of the amines and transfer these coordinates to CW and CCW 40 monomer helical models.

Molecular Dynamics Simulations. MD simulations of 20 ns on CW and CCW helical conformations and polymer amine complexes were carried out using GROMACS 2019.^{48,49} Polymer and amines were parametrized using AmberTools19⁵⁰ applying the General Amber Force Field (GAFF)⁵¹ and the AM1 BCC method for RESP charges.⁵² The 40 monomer helical models were solvated using a pre equilibrated cubic box of DMSO molecules provided by Caleman et al. and their solvent database,⁵³ and sodium counterions were added to the

pure polymer simulations. The systems were minimized and then equilibrated in two steps using the NVT and NPT ensembles considering position restraint using LINCS⁵⁴ to constrain all bonds of the polymer. During the NVT step, with 500 ps, a 2 fs time step using the V scale method⁵⁵ was used to control the temperature. The NPT equilibration step was performed under 500 ps with a 2 fs time step and the Parrinello–Rahman pressure coupling method.⁵⁶ Finally, a 20 ns MD production with periodic boundary conditions was performed using the V scale method⁵⁵ to keep the temperature at 300 K and the Parrinello–Rahman pressure coupling method⁵⁶ to keep the pressure at 1 atm. Electrostatic and van der Waals short range interactions were calculated with the Verlet method⁵⁷ with a cutoff of 1.4 nm. The long range electrostatic interaction was taken under the Particle Mesh Ewald (PME) method.⁵⁸ MD simulations for 40 monomer polymer amine complexes were carried out with the same conditions and settings.

III. RESULTS AND DISCUSSION

Helical Model and Polymer-Amine Complex Stability.

As shown above, dynamic helical polymers are challenging to study because their geometric helical configurations are difficult to distinguish experimentally. A helix structure can be constructed by arranging repeated monomer units per turn. The notation of $A * u/l$ is frequently used, where A is the class according to A chain motifs of the helix with u motifs per l repeating units.⁵⁹ DFT scan dihedral calculations on a dimer of a polyacetylene backbone with different degrees of side chain substitution were performed to observe energy differences in the twist of the dihedral formed by the single bond adjacent to two double bonds as displayed in panel (a) of Figure 2.

According to the experimental results obtained by Maeda et al.,²¹ carboxylate groups ($-\text{COO}^-$) in every side chain were considered in our models since they observed intensity changes in IR signals from $-\text{COOH}$ to $-\text{COO}^-$ groups when the helix is induced suggesting that the helical conformation on poly 1 is not possible without the presence of the negative carboxy charged groups.

In panel (a) of Figure 2, while adding 4 carboxyphenyl (4 CaPhe) groups to the polyacetylene backbone, the energy profile shows different local minima resulting in different possible poly 1 conformations. *Cis transoid* and *cis cisoid* conformations were found.

Assuming that the perfect *cis transoid* confirmation is obtained when the dihedral angles of the backbone are 180° and -180° , this local minimum moves to the values of 145° and -145° when attaching 4 CaPhe side chains to the backbone, resulting in a 2/1 helix (panel (a) of Figure 2). On the other hand, *cis-cisoid* conformations for negatively charged poly 1 were found at 54° and -54° resulting in a 3/1 helix shown in panels (b) and (c) of Figure 2. The difference in the backbone dihedral angle between the local minimum of the pure polyacetylene backbone and the dimer with 4 CaPhe substitutions may be due to the steric repulsion of the phenyl rings and the charge repulsion of the negative carboxylate groups. We found a low energy barrier of ca. 0.1 eV which makes reversions in the screw sense of the polymer from 145° to -145° possible.

In order to test the stability of these conformations, polymer models of *cis transoid* of 40 monomers for CW and CCW were created using the results from the dihedral scans. Since the transition from *cis transoid* to *cis cisoid* is not entropically favorable^{22,60} and the transition was not observed during the helical induction experiments,¹⁰ further calculations were

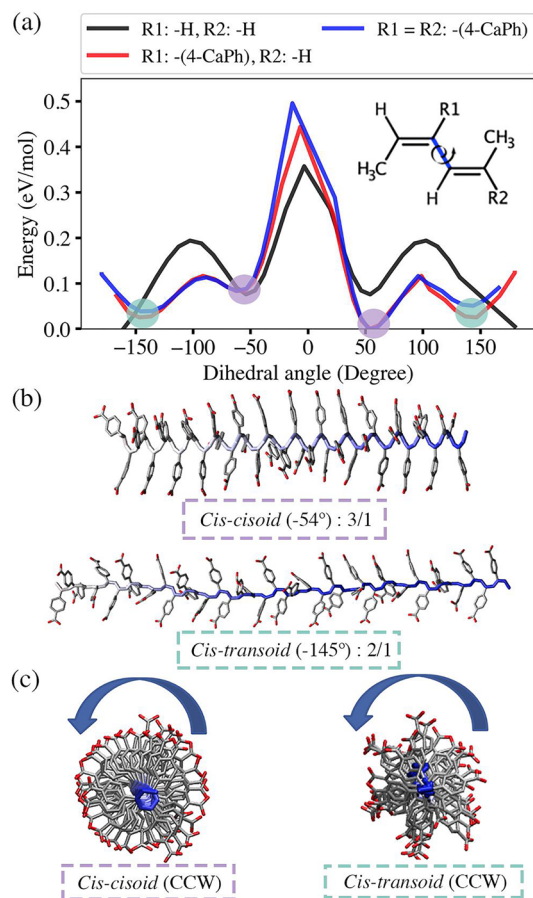


Figure 2. (a) Dihedral energy potential obtained from DFT scan calculations with different degrees of substitution of the dimer of polyacetylene. (b) Helical models created from the DFT scan information obtained for the CCW screw sense, *cis cisoid* and *cis transoid* conformations. (c) Upper view of helical models for the CCW screw sense.

limited to the *cis transoid* conformation. From dihedral scans, we obtained both CW and CCW models. The stability during the MD simulations of each helical polymer was based on Root Mean Square deviation (RMSD, shown in S11 available in the Supporting Information) and the Helical Index Error (HIE) (eq 6). This equation considers the deviation of dihedral angles during the simulation concerning an ideal model ($\phi_{model} - \phi_{simulation}$), and the range of angles in the local minimum obtained from the DFT scan studies where the helices start to lose their helicity is $\Delta\phi_{helix}$.

$$HIE = 1 - \tanh\left(\frac{\phi_{model} - \phi_{simulation}}{\Delta\phi_{helix}}\right)^2 \quad (6)$$

Panel (a) in Figure 3 shows the HIE values for helical models in the poly 1 CW and CCW screw senses. Its oscillatory behavior reveals the flexible nature of poly 1, presenting reversals along the polymer backbone, which is in agreement with the results of the polymer simulations by Yashima in 1997¹⁰ when simulating 20 monomer poly 1 but with neutral carboxylic groups. Additionally, dihedral angles per monomer of the backbone polymer were obtained by taking the average of dihedral values (S12 and their occurrence in S13 as shown in the Supporting Information). The occurrence of helical sense per

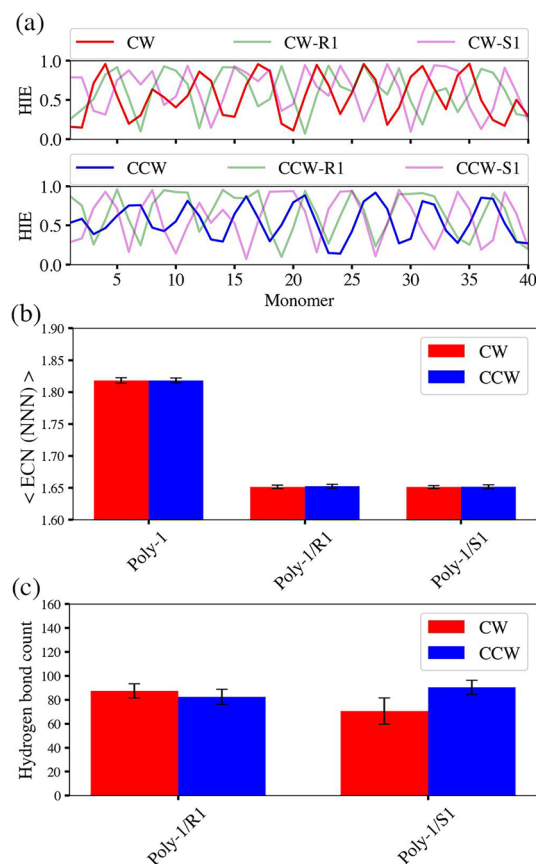


Figure 3. (a) Helical Index Error (HIE) obtained for CW (red) and CCW (blue) screw senses of poly 1. (b) The ECN (NNN) was calculated for each frame in a trajectory of 200 frames from our MD calculations, and then the global $\langle ECN \rangle$ was obtained. (c) Hydrogen bond count performed by amines and polymer during the MD simulations.

dihedral angle is computed by sorting the dihedral angles as CW for positive and CCW for negative.

While angles of 145° and -145° were obtained from the dihedral scan calculations for the best helical model, during the simulations, most of the dihedral average values moved toward ca. 160° and -160° . The results obtained for the dihedral angle occurrence clearly show the observed inversion of screw sense during the simulations without showing any preference for the CW or CCW sense.

To understand the role of chiral amines interacting with poly 1 in the helical stabilization in these chiral compounds, MD simulations of CW and CCW helical models interacting with R1 and S1 chiral compounds were carried out. R1 and S1 amines as depicted in Figure 1 were chosen for our simulations since they are chiral compounds with high intensity ICD bands²¹ at interacting with poly 1, and they present naphthalene rings as aromatic bulky groups, a feature notified as an essential factor for helical induction.¹⁰ Experimental results by Maeda et al.²¹ on helical induction of poly 1 using R1 and S1 revealed that the ion pair formation between the polymer side chains and amines is essential for the helix induction and to obtain one handedness excess. Additionally, it has been suggested that chiral amines might generate cooperative hydrogen bonds (HB) or bidentate type ion pair interactions after the basic amine group removes the proton from the carboxylic groups of each monomer.¹⁰

In order to incorporate this information and determine the starting conformations of the polymer amine complexes, several systems of 4 monomer poly 1 complexes with R1 and S1 interacting with poly 1 by ionic HB interaction were optimized using the DFT setup mentioned before to determine the lowest energy complexes to use as a reference. Different orientations of the groups attached to the chiral carbon (naphthalene and methyl groups) were considered in the screening. The lowest energy complexes found are CW R1 and CCW S1 complexes with a $\Delta E = 0.012$ eV between them. The optimized complex structures obtained showed the bidentate type ion pair interaction as described in Figure 1, green and pink boxes for CW R1 and CCW S1 complexes, respectively. These two compounds perform opposite orientations of naphthalene rings and methyl groups. Thus, the ligands' relative position optimized via DFT was used to create 40 monomer polymer amine complexes to feed the MD simulations.

The adopted starting configurations for R1 and S1 with 40 monomer polymer complexes are displayed in Figure 1. The simulation using 40 monomer poly 1 amine complexes presents the helical sense performed by the backbone, as well as the ligands around the helical sense going in the opposite direction to the backbone sense (Figure 1). As before we performed MD simulations of 20 ns and the trajectories were analyzed calculating the HIE in panels (a) and (b) of Figure 3, an average of torsion angles and dihedral occurrence to evaluate the integrity of the helical conformation are shown in the Supporting Information (Figures SI2 and SI3). HIE values for both screw senses interacting with R1 and S1 showed similar flexibility respecting poly 1 not interacting with chiral compounds. It is possible to identify the average of dihedral values that fluctuate around 160° and -160° for CW and CCW, respectively.

These results are very similar to our first MD simulations in the absence of chiral amines attached but distinct from the minimum energy dihedral values obtained from the DFT scan. After our MD simulations, the average dihedral values with their occurrence per screw sense (Supporting Information, Figures SI2 and SI3) reveal no difference between polymer R1 and polymer S1 complexes indicating the lack of a driving force that pushes the system to one helical sense.

To evaluate the binding of the amines of the polymer, the average of the Effective Coordination Number^{61,62} (ECN), relative to the number of nearest neighbors (NNNs), was calculated for every polymer amine complex in the MD simulations. As shown in panel (b) of Figure 3, we did not find any significant differences for the ECN values calculated for poly 1 interacting with R1 and S1, showing that their absorption is similar in all simulated complexes. As displayed in panel (c) of Figure 3, the count of hydrogen bonds (HBs) reveals that almost as many HBs are present per monomer, showing the high probability of a cooperative HB between the chiral compounds and the polymer.

We therefore conclude that the model employed in the MD simulation cannot distinguish between chiral compounds interacting with poly 1. Viscometric and theoretical studies have shown that poly 1 right and left handed helical conformations could be rapidly interconvertible, and it has been suggested that even though the chiral amines could perform predominant ion pair interactions, they could be changing the population of the configuration states of the polymer.^{21,63} It is challenging to model the complete induction process with MD due to the inherent time scale problem. Other

limitations, such as the classical force fields by construction, do not explicitly account for the intermolecular interactions that include polarization and charge transfer effects, which are well described for several systems in DFT using the appropriate van der Waals correction³⁶ or that could be overcome by advanced MD techniques such as Car-Parrinello MD^{64,65} or using nonconventional force fields such as multipolar force fields.^{66,67}

Polymer-Amine Dissociation Calculations and Charge Analysis. To overcome the limitations explained in the previous section, we resorted to the electronic structure calculations to evaluate the dissociation energy of every ligand interacting with every monomer using our 4 monomer poly 1 amine complexes obtained before, and the influence of the chiral center was accounted for by manually modifying the swap of the methyl groups connected to the chiral carbon by the hydrogen. In this strategy, we preserve the coordinates of the complex but with the opposite chiral amine identity. We computed the dissociation energy values of all complexes by analyzing the dissociation pathway using a thermodynamic cycle as given in eq 1. As can be seen in panels (c) and (d) of Figure 4, we denote each ligand as $X M$, where X is R1 or S1 and M is the monomer position where the ligand interacts with the 4 monomer polymer.

The data indicate that the optimized poly 1 amine complexes obtained (Figure 4) have the ion pair interaction between amines and polymer as the main stabilizing interaction, which is in agreement with the high counting of HB obtained in our previous MD simulations. The values of the dissociation energy of each complex exhibit an affinity trend of R1 and S1 for CW and CCW helical senses, respectively (panels (a) and (b) of Figure 4 and the Supporting Information (Tables SI3 and SI4)). Such results are intuitive since the dissociation energy values obtained are directly related to the exchange of the methyl groups in the chiral center, meaning that the bidentate type interaction becomes geometrically less favorable.

This agrees with the distance values of hydrogen-oxygen displayed in Table 1, where the second HB performed by ligands S1 1 and S1 2 in the CW helical sense and particularly with R1 1 and R1 2 in the CCW helical sense increases compared with the lowest energy complexes found.

Experimental results from Maeda et al.²¹ using titration and IR spectra analysis showed ion pair interactions play a major role in the helical induction of poly 1. Their conclusions are in good agreement with our DFT results, in particular when analyzing HB distances of the CCW R1 and CCW S1 systems. The HB distance values obtained for acceptor proton (C-O... H) for CCW R1 are lower than for CCW S1, hence the nature of the amines and carboxylic groups is closer to neutral species for CCW R1 than ionic like in the case for CCW S1.

On the other hand, the differences in the absolute values of ΔE_{diss} obtained are explained by the differences in the HB interactions, and also in the case of the CCW R1 complex by the aromatic interaction of R1 2 and R1 4 ligands being lost, see panel (d) of Figure 4 affecting this result significantly as shown in panel (b) of Figure 4.

The dissociation energy shows a clear trend in the affinity of R1 and S1 for the clockwise and counterclockwise screw senses of poly 1, respectively. However, it does not point out where this interaction happens in the 4 monomer polymer amine complexes. To clarify this point, we performed a Bader charge analysis to determine the nature of the interaction in polymer amine in the complexes. The values obtained for the 4 monomer poly 1 for all the complexes are illustrated in Figure 4 with a color scale. Figure 4 shows that the Bader charge distribution

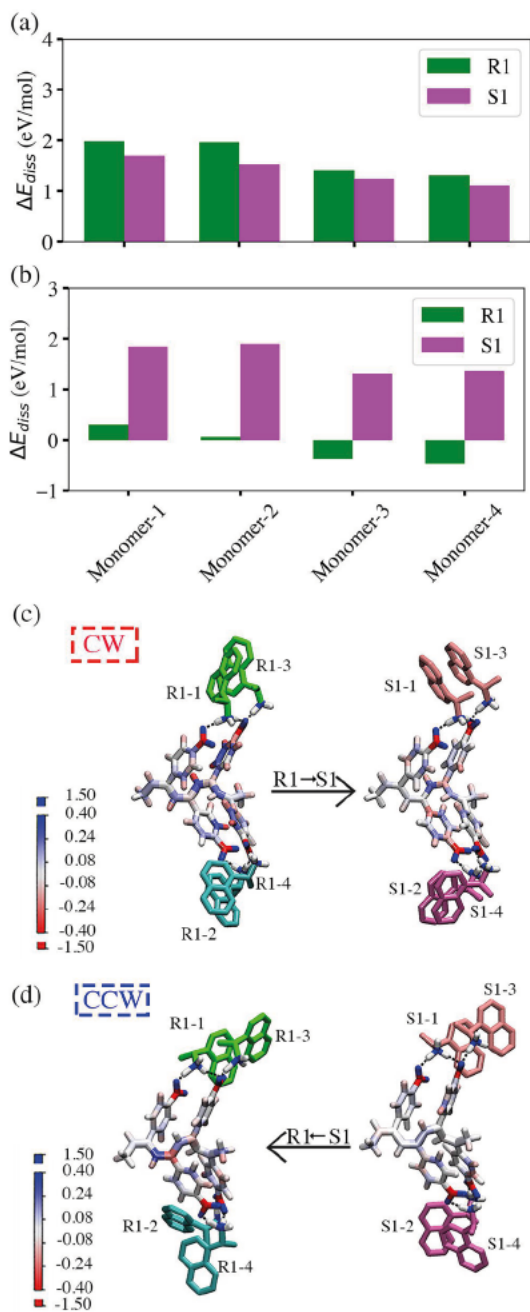


Figure 4. Values of ΔE_{diss} calculated with DFT for CW (a) and CCW (b) helix senses. Distribution of Bader net atomic charges on the poly 1 CW sense (c) and CCW sense (d) interacting with R1 and S1 chiral amines. R1 ligands are represented with green and cyan, while S1 ligands are represented with pink and magenta.

along with the complexes that R1 and S1 influence different effects over the backbone. We observe that R1 promotes a more significant charge in the backbone carbons of poly 1 than S1. Since this effect is observed in both helix senses, it could contribute to the stabilization of the complex or be part of the helical induction. On the other hand, the values obtained for the chiral carbon, nitrogen, and oxygen involved in the ion pair interaction between the polymer and the amines showed significant differences, confirming that the local effects play a prominent role in the stabilization. The values summarized in Table 2 show opposite trends when we compare amines in the

Table 1. Values of HB Performed by Chiral Amines with 4 Monomer Poly 1

amine-monomer	helix screw-sense	type of bond distance	first HB ^a (Å)	second HB ^b (Å)
R1-1	CW	N H	1.11	1.06
		C O H	1.49	1.68
R1-2	CW	N H	1.11	1.06
		C O H	1.48	1.69
R1-3	CW	N H	1.12	
		C O H	1.48	
R1-4	CW	N H	1.12	
		C O H	1.48	
S1-1	CW	N H	1.15	1.05
		C O H	1.40	1.77
S1-2	CW	N H	1.14	1.05
		C O H	1.40	1.77
S1-3	CW	N H	1.14	
		C O H	1.44	
S1-4	CW	N H	1.14	
		C O H	1.40	
R1-1	CCW	N H	1.56	1.02
		C O H	1.05	2.21
R1-2	CCW	N H	1.58	1.04
		C O H	1.05	1.93
R1-3	CCW	N H	1.64	
		C O H	1.04	
R1-4	CCW	N H	1.58	
		C O H	1.05	
S1-1	CCW	N H	1.13	1.05
		C O H	1.43	1.72
S1-2	CCW	N H	1.10	1.06
		C O H	1.52	1.68
S1-3	CCW	N H	1.11	
		C O H	1.54	
S1-4	CCW	N H	1.11	
		C O H	1.50	

^aMain HB performed with the monomer. ^bSecond HB performed with the next neighbor monomer.

Table 2. Bader Charge Values for Atoms Involved in the Ion Pair (Chiral Carbon, Nitrogen, and Oxygen)

atoms	CW-R1	CW-S1	CCW-R1	CCW-S1
chiral carbon	0.83	1.05	1.28	0.87
nitrogen	7.13	6.98	6.40	7.00
oxygen	9.06	9.25	10.70	9.12

same helical sense. One notes that nitrogen has a significant charge in CW R1 and CCW S1 and the opposite trend in the case of oxygen. These phenomena could be possible to the differences in the cooperative HB performed by the amines explained before. It is well known that the strength of acids and bases could be affected by aprotic polar solvents like DMSO.⁶⁸ However, the basicity of the amines could also be affected by the interaction displayed with different screw senses of the polymer reflected in the values of the Bader charges, as shown in Table 2.

IV. CONCLUSION

The helical induction on dynamic helical polymers such as the PPA polymer family has been extensively reported in the literature but not deeply understood. MD simulations cannot describe the helical induction nature due to its limitations, as we previously discussed. Despite our MD trajectories not being able

to provide useful information regarding the helical induction, the data obtained could provide useful information for future investigations in the field of high dynamic helical polymers. On the other hand, our DFT calculation results show that charge, chiral nature, and spatial orientation are crucial in helical induction because they enhance or diminish the bidentate type interactions. This agrees with the experimental results discussed by Yashima et al.,¹⁰ where they tried different chiral center positions away from the amino group yielding unclear ICD signals. Structural analysis of the contact interactions between the amines and polymer and Bader charge analysis gave essential insights to understand the nature of these complexes' screw sense, affinity, and stabilization. The findings in this work will be of interest to understand other dynamic helical polymers that experimental techniques struggle to probe.

V. DATA AND SOFTWARE AVAILABILITY

All the DFT calculations were carried out using TURBOMOLE 7.3³⁰ (<http://www.turbomole.com>). The creation of conformers for the scan calculations were generated using the open source PyMOL Application Programming Interface (API)⁶⁹ (<https://github.com/schrodinger/pymol-open-source>). The initial coordinates of 4 monomer polymer amine complexes were obtained manually starting with a hydrogen bond interaction between amines and carboxylate groups with different methyl and naphthalene group orientations. Bader charge analysis on polymer amine complexes was performed using the Workflow Active Nodes DFT VASP developed within the SimStack workflow framework^{46,47} (<https://github.com/KIT-Workflows/DFT-VASP>). Polymer structures were created using *AmberTools19* scripts using *tLeap* (<https://ambermd.org>), and the 4 monomer CW and CCW structures obtained from DFT calculations were used as a reference structure for charge calculations with *anteChamber*. Then, Amber input files were converted into GROMACS input files using *AcPype*⁷⁰ (<https://github.com/alanwilter/acpype>). First coordinates for 40 monomer polymer amine complexes were obtained using the DFT 4 monomer complexes as a reference and extended to the 40 monomer polymers using PyMOL API. MD simulations were initialized using GROMACS (<https://www.gromacs.org>) preprocessor tools with a pre-equilibrated solvation box of DMSO from Coleman et al.⁵³ Finally, simulations were performed using the GROMACS *mdrun* module. Visualization and pictures were made using Visual Molecular Dynamics (VMD) (<https://www.ks.uiuc.edu/Research/vmd>).

ASSOCIATED CONTENT

Supporting Information

The Supporting Information is available free of charge at <https://pubs.acs.org/doi/10.1021/acs.jcim.1c01347>.

Root mean square deviation analysis of all polymer structures during MD simulations, detailed information on behavior of dihedral angles along polymer during MD simulations, dissociation energy values obtained from DFT calculations for 4 monomer polymer-amine complexes, and values of Bader atomic charges for 4 monomer polymer-amine complexes (PDF)

PDB structures of 4 and 40 monomer complexes with R1 and S1 ligands (ZIP)

AUTHOR INFORMATION

Corresponding Authors

Montserrat Penaloza Amion – *Institute of Nanotechnology Hermann von Helmholtz Platz, Karlsruhe Institute of Technology, 76021 Karlsruhe, Germany*; orcid.org/0000-0003-4241-6904; Email: montserrat.amion@kit.edu

Celso R. C. Rêgo – *Institute of Nanotechnology Hermann von Helmholtz Platz, Karlsruhe Institute of Technology, 76021 Karlsruhe, Germany*; orcid.org/0000-0003-1861-2438; Email: celso.rego@kit.edu

Wolfgang Wenzel – *Institute of Nanotechnology Hermann von Helmholtz Platz, Karlsruhe Institute of Technology, 76021 Karlsruhe, Germany*; orcid.org/0000-0001-9487-4689; Email: wolfgang.wenzel@kit.edu

Notes

The authors declare no competing financial interest.

ACKNOWLEDGMENTS

This research was funded by the Deutscher Akademischer Austauschdienst (DAAD) with the scholarship of M.P. A. (91683960) and the Deutsche Forschungsgemeinschaft (DFG, German Research Foundation) within Collaborative Research Centre (SFB) 1176 "Molecular Structuring of Soft Matter" (project Q3). W.W. acknowledges the financial support by the GRK 2450 "Scale bridging methods in computational nano science" project and the Deutsche Forschungsgemeinschaft (DFG, German Research Foundation) under Germany's Excellence Strategy – 2082/1 – 390761711 (3DMM2O, Thrust A3). C.R.C.R. and W.W. thank the German Federal Ministry of Education and Research (BMBF) for financial support of the project Innovation Platform MaterialDigital (www.materialdigital.de) through project funding FKZ no. 13XP5094A.

REFERENCES

- (1) Yashima, E.; Maeda, K.; Iida, H.; Furusho, Y.; Nagai, K. Helical Polymers: Synthesis, Structures, and Functions. *Chem. Rev.* 2009, 109, 6102–6211.
- (2) Jeong, B.; Gutowska, A. Lessons from nature: stimuli responsive polymers and their biomedical applications. *Trends Biotechnol.* 2002, 20, 305–311.
- (3) Miyata, T.; Uragami, T.; Nakamae, K. Biomolecule sensitive hydrogels. *Adv. Drug Delivery Rev.* 2002, 54, 79–98.
- (4) Kikuchi, A.; Okano, T. Intelligent thermoresponsive polymeric stationary phases for aqueous chromatography of biological compounds. *Prog. Polym. Sci.* 2002, 27, 1165–1193.
- (5) Gil, E.; Hudson, S. Stimuli responsive polymers and their bioconjugates. *Prog. Polym. Sci.* 2004, 29, 1173–1222.
- (6) Okamoto, Y.; Suzuki, K.; Ohta, K.; Hatada, K.; Yuki, H. Optically active poly(triphenylmethyl methacrylate) with one handed helical conformation. *J. Am. Chem. Soc.* 1979, 101, 4763–4765.
- (7) Nolte, R. J. M.; Van Beijnen, A. J. M.; Drenth, W. Chirality in polyisocyanides. *J. Am. Chem. Soc.* 1974, 96, 5932–5933.
- (8) Yashima, E. Synthesis and structure determination of helical polymers. *Polym. J.* 2010, 42, 3–16.
- (9) Yashima, E.; Matsushima, T.; Okamoto, Y. Poly((4-carboxyphenyl)acetylene) as a Probe for Chirality Assignment of Amines by Circular Dichroism. *J. Am. Chem. Soc.* 1995, 117, 11596–11597.
- (10) Yashima, E.; Matsushima, T.; Okamoto, Y. Chirality Assignment of Amines and Amino Alcohols Based on Circular Dichroism Induced

by Helix Formation of a Stereoregular Poly((4 carboxyphenyl) acetylene) through Acid–Base Complexation. *J. Am. Chem. Soc.* **1997**, *119*, 6345–6359.

(11) Green, M. M.; Reidy, M. P.; Johnson, R. D.; Darling, G.; O’Leary, D. J.; Willson, G. Macromolecular stereochemistry: the out of proportion influence of optically active comonomers on the conformational characteristics of polyisocyanates. The sergeants and soldiers experiment. *J. Am. Chem. Soc.* **1989**, *111*, 6452–6454.

(12) Green, M. M.; Garetz, B. A.; Munoz, B.; Chang, H.; Hoke, S.; Cooks, R. G. Majority Rules in the Copolymerization of Mirror Image Isomers. *J. Am. Chem. Soc.* **1995**, *117*, 4181–4182.

(13) Yashima, E.; Maeda, K.; Okamoto, Y. Memory of macromolecular helicity assisted by interaction with achiral small molecules. *Nature* **1999**, *399*, 449–451.

(14) Morino, K.; Watase, N.; Maeda, K.; Yashima, E. Chiral Amplification in Macromolecular Helicity Assisted by Noncovalent Interaction with Achiral Amines and Memory of the Helical Chirality. *Chem. Eur. J.* **2004**, *10*, 4703–4707.

(15) Onouchi, H.; Kashiwagi, D.; Hayashi, K.; Maeda, K.; Yashima, E. Helicity Induction on Poly(phenylacetylene)s Bearing Phosphonic Acid Pendants with Chiral Amines and Memory of the Macromolecular Helicity Assisted by Interaction with Achiral Amines in Dimethyl Sulfoxide. *Macromolecules* **2004**, *37*, 5495–5503.

(16) Onouchi, H.; Hasegawa, T.; Kashiwagi, D.; Ishiguro, H.; Maeda, K.; Yashima, E. Helicity Induction in Charged Poly(phenylacetylene)s Bearing Various Acidic Functional Groups in Water and Its Mechanism. *Macromolecules* **2005**, *38*, 8625–8633.

(17) Onouchi, H.; Miyagawa, T.; Furuko, A.; Maeda, K.; Yashima, E. Enantioselective Esterification of Prochiral Phosphonate Pendants of a Polyphenylacetylene Assisted by Macromolecular Helicity: Storage of a Dynamic Macromolecular Helicity Memory. *J. Am. Chem. Soc.* **2005**, *127*, 2960–2965.

(18) Nagai, K.; Maeda, K.; Takeyama, Y.; Sakajiri, K.; Yashima, E. Helicity Induction and Chiral Amplification in a Poly(phenylacetylene) Bearing N, N Diisopropylaminomethyl Groups with Chiral Acids in Water. *Macromolecules* **2005**, *38*, 5444–5451.

(19) Morino, K.; Oobo, M.; Yashima, E. Helicity Induction in a Poly(phenylacetylene) Bearing Aza 18 crown 6 Ether Pendants with Optically Active Bis(amino acid)s and Its Chiral Stimuli Responsive Gelation. *Macromolecules* **2005**, *38*, 3461–3468.

(20) Kobayashi, S.; Morino, K.; Yashima, E. Macromolecular helicity inversion of an optically active helical poly(phenylacetylene) by chemical modification of the side groups. *Chem. Commun.* **2007**, 2351–2353.

(21) Maeda, K.; Morino, K.; Okamoto, Y.; Sato, T.; Yashima, E. Mechanism of Helix Induction on a Stereoregular Poly((4 carboxyphenyl)acetylene) with Chiral Amines and Memory of the Macromolecular Helicity Assisted by Interaction with Achiral Amines. *J. Am. Chem. Soc.* **2004**, *126*, 4329–4342.

(22) Percec, V.; Rudick, J. G.; Peterca, M.; Wagner, M.; Obata, M.; Mitchell, C. M.; Cho, W. D.; Balagurusamy, V. S. K.; Heiney, P. A. Thermoreversible Cis – Cisoidal to Cis – Transoidal Isomerization of Helical Dendronized Polyphenylacetylenes. *J. Am. Chem. Soc.* **2005**, *127*, 15257–15264.

(23) Suárez Picado, E.; Quiñoá, E.; Riguera, R.; Freire, F. Poly(phenylacetylene) Amines: A General Route to Water Soluble Helical Polyamines. *Chem. Mater.* **2018**, *30*, 6908–6914.

(24) Christofferson, A. J.; Yiapanis, G.; Ren, J. M.; Qiao, G. G.; Satoh, K.; Kamigaito, M.; Yarovsky, I. Molecular mapping of poly(methyl methacrylate) super helix stereocomplexes. *Chem. Sci.* **2015**, *6*, 1370–1378.

(25) Liu, W.; Luo, X.; Bao, Y.; Liu, Y. P.; Ning, G. H.; Abdelwahab, I.; Li, L.; Nai, C. T.; Hu, Z. G.; Zhao, D.; Liu, B.; Quek, S. Y.; Loh, K. P. A two dimensional conjugated aromatic polymer via C–C coupling reaction. *Nat. Chem.* **2017**, *9*, 563–570.

(26) Huang, X.; Zhang, X.; Ren, G. K.; Jiang, J.; Dan, Z.; Zhang, Q.; Zhang, X.; Nan, C. W.; Shen, Y. Non intuitive concomitant enhancement of dielectric permittivity, breakdown strength and energy density

in percolative polymer nanocomposites by trace Ag nanodots. *J. Mater. Chem. A* **2019**, *7*, 15198–15206.

(27) Pham, T. L. M.; Phung, K. T.; Ho, T. V.; Le, T. A.; Nguyen, A. T. T. Density functional theory insights into the bonding of CH₃OH and CH₃O with Ir(111) surface. *Sci. Technol. Dev. J.* **2021**, *24*, 833.

(28) Wildman, J.; Repiščák, P.; Paterson, M. J.; Galbraith, I. General Force Field Parametrization Scheme for Molecular Dynamics Simulations of Conjugated Materials in Solution. *J. Chem. Theory Comput.* **2016**, *12*, 3813–3824.

(29) Ryde, U.; Söderhjelm, P. Ligand Binding Affinity Estimates Supported by Quantum Mechanical Methods. *Chem. Rev.* **2016**, *116*, 5520–5566.

(30) TURBOMOLE V7.3; TURBOMOLE GmbH: 2018; a development of University of Karlsruhe and Forschungszentrum Karlsruhe GmbH, 1989–2007, since 2007. Available from <http://www.turbomole.com> (accessed 2022 01 24).

(31) Furche, F.; Ahlrichs, R.; Hättig, C.; Klopper, W.; Sierka, M.; Weigend, F. Turbomole. *Wiley Interdiscip. Rev.: Comput. Mol. Sci.* **2014**, *4*, 91–100.

(32) Balasubramani, S. G.; Chen, G. P.; Coriani, S.; Diedenhofen, M.; Frank, M. S.; Franzke, Y. J.; Furche, F.; Grotjahn, R.; Harding, M. E.; Hättig, C.; Hellweg, A.; Helmich Paris, B.; Holzer, C.; Huniar, U.; Kaupp, M.; Marefat Khah, A.; Karbalaei Khani, S.; Müller, T.; Mack, F.; Nguyen, B. D.; Parker, S. M.; Perlt, E.; Rappoport, D.; Reiter, K.; Roy, S.; Rückert, M.; Schmitz, G.; Sierka, M.; Tapavicza, E.; Tew, D. P.; van Wüllen, C.; Voora, V. K.; Weigend, F.; Wodyński, A.; Yu, J. M. TURBOMOLE: Modular program suite for *ab initio* quantum chemical and condensed matter simulations. *J. Chem. Phys.* **2020**, *152*, 184107.

(33) Becke, A. D. A new mixing of Hartree–Fock and local density functional theories. *J. Chem. Phys.* **1993**, *98*, 1372–1377.

(34) Becke, A. D. Density functional thermochemistry. III. The role of exact exchange. *J. Chem. Phys.* **1993**, *98*, 5648–5652.

(35) Zheng, J.; Xu, X.; Truhlar, D. G. Minimally augmented Karlsruhe basis sets. *Theor. Chem. Acc.* **2011**, *128*, 295–305.

(36) Rêgo, C. R. C.; Oliveira, L. N.; Tereshchuk, P.; Silva, J. L. F. D. Comparative study of van der Waals corrections to the bulk properties of graphite. *J. Phys.: Condens. Matter* **2015**, *27*, 415502.

(37) Rêgo, C. R. C.; Oliveira, L. N.; Tereshchuk, P.; Silva, J. L. F. D. Corrigendum: Comparative study of van der Waals corrections to the bulk properties of graphite (2015). *J. Phys.: Condens. Matter* **2016**, *28*, 129501.

(38) Grimme, S.; Antony, J.; Ehrlich, S.; Krieg, H. A consistent and accurate *ab initio* parametrization of density functional dispersion correction (DFT-D) for the 94 elements H–Pu. *J. Chem. Phys.* **2010**, *132*, 154104.

(39) Grimme, S.; Ehrlich, S.; Goerigk, L. Effect of the damping function in dispersion corrected density functional theory. *J. Comput. Chem.* **2011**, *32*, 1456–1465.

(40) Schäfer, A.; Klamt, A.; Sattler, D.; Lohrenz, J. C. W.; Eckert, F. COSMO Implementation in TURBOMOLE: Extension of an efficient quantum chemical code towards liquid systems. *Phys. Chem. Chem. Phys.* **2000**, *2*, 2187–2193.

(41) Blöchl, P. E. Projector augmented wave method. *Phys. Rev. B* **1994**, *50*, 17953–17979.

(42) Kresse, G.; Joubert, D. From ultrasoft pseudopotentials to the projector augmented wave method. *Phys. Rev. B* **1999**, *59*, 1758–1775.

(43) Kresse, G.; Furthmüller, J. Efficient iterative schemes for ab initio total energy calculations using a plane wave basis set. *Phys. Rev. B* **1996**, *54*, 11169–11186.

(44) Hafner, J. *Ab initio* simulations of materials using VASP: Density functional theory and beyond. *J. Comput. Chem.* **2008**, *29*, 2044–2078.

(45) Tang, W.; Sanville, E.; Henkelman, G. A grid based Bader analysis algorithm without lattice bias. *J. Phys.: Condens. Matter* **2009**, *21*, 084204.

(46) Rêgo, C. R. C. KIT Workflows/DFT VASP: DFT VASP, 2021. Available from <https://github.com/KIT-Workflows/DFT-VASP> (accessed 2022 01 24).

- (47) Schaarschmidt, J. Workflow Engineering in Materials Design within the BATTERY 2030+ Project. *Adv. Energy Mater.* **2021**, 2102638.
- (48) Berendsen, H. J.; van der Spoel, D.; van Drunen, R. GROMACS: a message passing parallel molecular dynamics implementation. *Comput. Phys. Commun.* **1995**, *91*, 43–56.
- (49) Abraham, M. J.; Murtola, T.; Schulz, R.; Páll, S.; Smith, J. C.; Hess, B.; Lindahl, E. GROMACS: High performance molecular simulations through multi level parallelism from laptops to super computers. *SoftwareX* **2015**, *1–2*, 19–25.
- (50) Duke, R.; Giese, T.; Gohlke, H.; Goetz, A.; Homeyer, N.; Izadi, S.; Janowski, P.; Kaus, J.; Kovalenko, A.; Lee, T. et al. *AmberTools 16*; University of California: San Francisco, 2016.
- (51) Ozipinar, G. A.; Peukert, W.; Clark, T. An improved generalized AMBER force field (GAFF) for urea. *J. Mol. Model.* **2010**, *16*, 1427–40.
- (52) Jakalian, A.; Bush, B. L.; Jack, D. B.; Bayly, C. I. Fast, efficient generation of high quality atomic charges. AM1 BCC model: I. Method. *J. Comput. Chem.* **2000**, *21*, 132–146.
- (53) Caleman, C.; van Maaren, P. J.; Hong, M.; Hub, J. S.; Costa, L. T.; van der Spoel, D. Force Field Benchmark of Organic Liquids: Density, Enthalpy of Vaporization, Heat Capacities, Surface Tension, Isothermal Compressibility, Volumetric Expansion Coefficient, and Dielectric Constant. *J. Chem. Theory Comput.* **2012**, *8*, 61–74.
- (54) Hess, B.; Bekker, H.; Berendsen, H. J.; Fraaije, J. G. LINCS: a linear constraint solver for molecular simulations. *J. Comput. Chem.* **1997**, *18*, 1463–1472.
- (55) Bussi, G.; Donadio, D.; Parrinello, M. Canonical sampling through velocity rescaling. *J. Chem. Phys.* **2007**, *126*, 014101.
- (56) Parrinello, M.; Rahman, A. Polymorphic transitions in single crystals: A new molecular dynamics method. *J. Appl. Phys.* **1981**, *52*, 7182–7190.
- (57) Swope, W. C.; Andersen, H. C.; Berens, P. H.; Wilson, K. R. A computer simulation method for the calculation of equilibrium constants for the formation of physical clusters of molecules: Application to small water clusters. *J. Chem. Phys.* **1982**, *76*, 637–649.
- (58) Darden, T.; York, D.; Pedersen, L. Particle mesh Ewald: An $N - \log(N)$ method for Ewald sums in large systems. *J. Chem. Phys.* **1993**, *98*, 10089–10092.
- (59) Wunderlich, B. *Macromolecular physics. Crystal structure, morphology, defects*; Academic Press: 1973; Vol. 1, DOI: [10.1016/B978-0-12-765601-4.50008-1](https://doi.org/10.1016/B978-0-12-765601-4.50008-1).
- (60) Wang, S.; Feng, X.; Zhao, Z.; Zhang, J.; Wan, X. Reversible *Cis Cisoid* to *Cis Transoid* Helical Structure Transition in Poly(3,5 disubstituted phenylacetylene)s. *Macromolecules* **2016**, *49*, 8407–8417.
- (61) Hoppe, R. Effective coordination numbers (ECoN) and mean Active fictive ionic radii (MEFIR). *Z. Kristallogr. Cryst. Mater.* **1979**, *150*, 23–52.
- (62) Da Silva, J. L. F. Effective coordination concept applied for phase change (GeTe)_m(Sb₂Te₃)_n compounds. *J. Appl. Phys.* **2011**, *109*, 023502.
- (63) Ashida, Y.; Sato, T.; Morino, K.; Maeda, K.; Okamoto, Y.; Yashima, E. Helical Structural Change in Poly ((4 carboxyphenyl) acetylene) by Acid Base Complexation with an Optically Active Amine. *Macromolecules* **2003**, *36*, 3345–3350.
- (64) Hutter, J. Car–Parrinello molecular dynamics. *Wiley Interdiscip. Rev.: Comput. Mol. Sci.* **2012**, *2*, 604–612.
- (65) Stare, J.; Mavri, J.; Grdadolnik, J.; Zidar, J.; Maksić, Z. B.; Vianello, R. Hydrogen bond dynamics of histamine monocation in aqueous solution: Car–Parrinello molecular dynamics and vibrational spectroscopy study. *J. Phys. Chem. B* **2011**, *115*, 5999–6010.
- (66) Koner, D.; Salehi, S. M.; Mondal, P.; Meuwly, M. Non conventional force fields for applications in spectroscopy and chemical reaction dynamics. *J. Chem. Phys.* **2020**, *153*, 010901.
- (67) Mondal, P.; Cazade, P. A.; Das, A. K.; Bereau, T.; Meuwly, M. Multipolar Force Fields for Amide I Spectroscopy from Conformational Dynamics of the Alanine Trimer. *J. Phys. Chem. B* **2021**, *125*, 10928.
- (68) Anslyn, E. V.; Dougherty, D. A. *Modern physical organic chemistry*; University Science Books: 2006.
- (69) Schrödinger, L. L. C. *PyMOL Molecular Graphics System*, Version 1.8; 2015.
- (70) Sousa da Silva, A. W.; Vranken, W. F. ACPYPE Antechamber python parser interface. *BMC Res. Notes* **2012**, *5*, 367.